A R C H I V E O F M E C H A N I C A L E N G I N E E R I N G

Volume 68 2021 Number 4

DOI: 10.24425/ame.2021.139311

Key words: reciprocating compressor, crankshaft optimization, weight reduction, topology optimization, stress distribution, crank web, lightweight crankshaft design, crack modeling, static structural analysis, modal analysis.

Ali Arshad [1], Pengbo Cong [2],
Adham Ahmed Awad Elsayed Elmenshawy [1], Ilmārs Blumbergs [1]

Design optimization for the weight reduction of 2-cylinder reciprocating compressor crankshaft

This study aims to optimize the 2-cylinder in-line reciprocating compressor crankshaft. As the crankshaft is considered the "bulkiest" component of the reciprocating compressor, its weight reduction is the focus of current research for improved performance and lower cost. Therefore, achieving a lightweight crankshaft without compromising the mechanical properties is the core objective of this study. Computational analysis for the crankshaft design optimization was performed in the following steps: kinematic analysis, static analysis, fatigue analysis, topology analysis, and dynamic modal analysis. Material retention by employing topology optimization resulted in a significant amount of weight reduction. A weight reduction of approximately 13% of the original crankshaft was achieved. At the same time, design optimization results demonstrate improvement in the mechanical properties due to better stress concentration and distribution on the crankshaft. In addition, material retention would also contribute to the material cost reduction of the crankshaft. The exact 3D model of the optimized crankshaft with complete design features is the main outcome of this research. The optimization and stress analysis methodology developed in this study can be used in broader fields such as reciprocating compressors/engines, structures, piping, and aerospace industries.

1. Introduction

The crankshaft is considered the most important component of a reciprocating compressor/engine. In recent decades, weight reduction of the crankshaft has remained one of the core research goals in the fields of reciprocating systems. In

✉ Ali Arshad, e-mail: ali.arshad@rtu.lv

[1]Institute of Aeronautics, Faculty of Mechanical Engineering, Transport and Aeronautics, Riga Technical University, Latvia; ORCIDs: A.A.: 0000-0003-0317-9694; A.E.E: 0000-0001-9210-1463; I.B.: 0000-0003-0975-6771

[2]Institute of Mechanics and Mechanical Engineering, Faculty of Mechanical Engineering, Transport and Aeronautics, Riga Technical University, Latvia

terms of weight, the crankshaft of the reciprocating compression systems is, in fact, the "bulkiest" component due to its complex geometry which consists of several-cylinder journals and crank webs. In order to cope with such bulky characteristics, the weight optimization of the crankshaft is a beneficial approach that can contribute to reducing the relative manufacturing cost. In addition, smaller and lighter components are equally beneficial in reducing vibration and noise. For the automobile industry, the requirements of high fuel economy, low exhaust emissions, and high specific power can also be achieved at the same time [1].

The research on crankshaft weight optimization has been carried out since the inception of the reciprocating compressors and was the main focus of numerous past studies [1–7]; however, there is still a huge potential for further improvements in the optimized crankshaft lightweight designs. Druschitz [2] presented several lightweight crankshaft designs developed with the potential to provide a significant amount of weight reduction. The existing crankshaft lightweight methods mainly include hollow crankshaft design, use of innovative materials, and shape optimization such as optimizing the web design and smaller bearing diameter. In this regard, Honda R&D department [3] was the first to develop the hollow crankshaft for racing vehicle engines. Papadimitriou [4] deeply investigated the potential and feasibility of hallow crankshaft lightweight design in automotive engines and managed to reduce 20% crankshaft weight. The study further confirmed the scope for the hollow lightweight design. Although the use of hollow designs can achieve a good result in terms of mass reduction, this method usually leads to a decrease in stiffness and causes several serious concerns related to mechanical performance.

The use of innovative materials is another effective approach to achieve weight reduction. The new grades of steel or steel alloys with improved strength properties and lower weights are usually employed by the automotive industry to fulfill the weight reduction demands; as a result, the weight reduction can reach up to 25% [5]. On the other hand, shape optimization is generally based on genetic and evolutionary algorithms, thus, making it a relatively new area of research. Lampinen [6] studied the topology optimization application on a cam design to minimize the system vibration and keeping the changes smooth in the cam. Alberts [7] investigated the crankshaft lightweight optimization effect on different crank web profiles and managed to get a satisfactory weight as well as a reduction in imbalance.

The fundamental research on static and fatigue strength is the principle content for the crankshaft design. Static analysis is generally performed to ensure the stress distribution under the maximum permitted loads by identifying the sensitive sections. Henry [8] utilized FEM (Finite Element Method) and BEM (Boundary Element Method) on the crankshaft to investigate the stress concentration; the results were further used for the durability of the crankshaft and conceptual design.Guagliano [9] conducted a study on a marine diesel engine crankshaft in which two different FE (Finite Element) models were investigated. Due to the computational limitations for the 3D model, a 2D model was used to obtain the stress concentration factor, which showed accurate results for a centered load and

eccentric loads. Borges [10] conducted a FEM-based study on a geometrically restricted model of an automotive crankshaft. This study was based on static load analysis and investigated loading at a specific crank angle. The FE model results showed uniform stress distribution over the crank, and the only region with high-stress concentration was at the fillet between the crank-pin bearing and the crank web. Borges [10] analyzed the stress distribution on automotive engine crankshaft for stress homogenization and localization of stress concentration points. This study also concluded that the stress concentration was restricted to the fillet of the crankpin bearing.

Dynamic loads and rotating work conditions exert cyclic loading on the crankshaft, which is often responsible for fatigue failure. Therefore, fatigue strength is extremely important in mechanical analysis and design, especially when the structural components are under the influence of cyclic loading. Taylor [11] analyzed the crankshaft fatigue failure under the bending and torsional loads. The equivalent K method, also known as 'crack modeling', was employed to observe the stress concentration phenomenon in the crankshaft. It was observed that the finite element meshing quality played a significant effect on the stress analysis and the accuracy of the result prediction. Li [12] investigated the influences of chemical composition, mechanical properties, and macroscopic/microscopic features of the crankshaft failure. The study concluded that the fatigue fracture was only attributed to the fracture crack caused by bending stress concentration initiation and propagation. Mekar [13] conducted Linear Elastic Fracture Mechanics (LEFM) and Critical Distance Approach (CDA) to predict the probable position of the crack generation, which could further influence the crankshaft fatigue life. The results showed that all the critical positions were located at the fillet due to high-stress gradients. Shi [14] studied the crankshaft fatigue failure process, and the experimental results laid a foundation for the crankshaft remanufacturing. The study successfully investigated the crankshaft fatigue failure process, fatigue initiation, fatigue crack propagation (FCP), and fracture. For the dynamic analysis of the crankshaft, Yao [15] conducted a modal analysis using ANSYS on the crankshaft to observe the natural frequency and vibration modes. A 3D model was created for the analysis, and as a result, 20 order natural frequency and vibration modes were obtained to prevent the system resonance. Mendes [16] performed structural analysis on the crankshaft and crankcase to pursue better design in terms of stiffness with minimum changes in design. Yu [17] utilized a combination of flexible body dynamics and finite element analysis for the stress calculation in the compressor crankshaft, which could provide the load variation of the crank and connecting rod mechanism with time. The results indicated the maximum von Mises stress occurred at the fillet in the junction between crank pin and crank web and successfully predicted the crankshaft life by using the stress history.

Most of the previous research on the crankshaft was performed on the reciprocating engines by using hollow design and shape optimization; however, research performed on the compressor crankshaft is relatively limited. As mentioned earlier,

the crankshaft, due to its complex geometry, takes a large proportion of the total weight of the system; therefore, the core focus of this study is the crankshaft weight reduction of the reciprocating compressor using the topology optimization method with improved mechanical properties. The "ZW series LPG compressor" is chosen for this study due to its extensive use in industries, especially in Liquefied Petroleum Gas (LPG). Also, this compressor is one of the most successful compressors in the last few decades, which is widely used in fuel stations, domestic and business building heating, and even in the food courts for kitchen use. Reliability and performance also make it a potential candidate to stay for decades to come. In this paper, the optimization of the crankshaft is performed with the interchangeability precondition of the crankshaft, i.e., even after the design optimization the crankshaft should still be suitable to be used in the parent compressor system. Crankshaft optimization is carried out in the following steps: (1) mechanism analysis, (2) static analysis, (3) fatigue analysis, (4) topology analysis, (5) dynamic modal analysis. Commercially available ANSYS software was used for the static and dynamic analysis, whereas for the kinematic analysis ADMAS was utilized. Description of the base reciprocating compressor and crankshaft parameters is followed by the details of the crankshaft design, their configuration, and computational schemes. Numerical results manifested a significant reduction in the crankshaft weight, which is approximately 13% lighter as compared to the base crankshaft model. In addition, the stress and deformation distribution on the optimized model were also improved.

This paper is part of the series of the current [18–23] and future studies under the ERDF (European Regional Development Fund) project, which aims at developing educational/research purpose high-speed flow testing facilities and aerospace equipment at Riga Technical University, Latvia. The findings and methods learned during this work will be utilized in the mechanical design and structural testing of the sensitive parts and equipment, especially for the compression system of the wind tunnel.

2. Computational modeling

2.1. Reciprocating compressor specifications

At first, the reciprocating compressor host was modeled in SOLIDWORKS; the host model will only be used for the mechanism analysis. The layout of the compressor host and important operating parameters of the reciprocating compressor are summarized in Fig. 1 and Table 1, respectively. The compressor host is driven by the external electrical motor through the crankshaft; the crankshaft then transfers the power to the piston through the connecting rod by which the cylinder gas volume changes, resulting in high-pressure gas supply from the compressor.

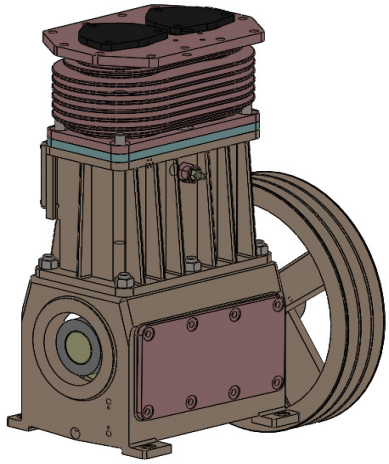

Fig. 1. Layout of the compressor host

Table 1.

Performance Parameters of Compressor [24]

Compressible Medium	LPG
Standard Capacity (m^3/min)	0.8
Rotational Speed (r/min)	550
Suction Pressure (MPa)	1
Exhaust Pressure (MPa)	1.6
Suction Temperature (°)	$\leqslant 50$
Exhaust Temperature (°)	$\leqslant 110$

2.2. Crankshaft modeling and properties

The reciprocating compressor crankshaft consists of two-rod journals; the total length of the crankshaft is 460 mm, while the total weight is 14826.54 g. The computational model of the original crankshaft was created in SOLIDWORKS and is shown in Fig. 2. Important mechanical properties of the crankshaft are presented in Table 2.

Table 2.

Mechanical properties of crankshaft

Elastic modulus (N/m^2)	$2.05 \cdot 10^{11}$
Anti-shear modulus (N/m^2)	$8.0 \cdot 10^{10}$
Poisson ratio	0.3
Density (kg/m^3)	7850
Tension strength (N/m^2)	$6.25 \cdot 10^8$
Yield strength (N/m^2)	$5.3 \cdot 10^8$

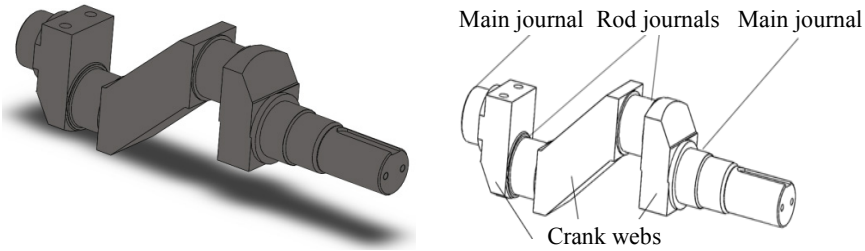

(a) Initial position (b) Final position

Fig. 2. Crankshaft model

3. Mechanism analysis

A kinematic analysis deals with the motion in terms of displacement, velocity, and acceleration without the inclusion of forces. Fundamental and theoretical details of the kinematic analysis can be found in Ref. [25]. For the study of the motion mechanism of the reciprocating compressor, the crank mechanism in ADAMS/View software was utilized. Kinematic analysis was performed by simulating the assembled 3D model of the crank mechanism, as shown in Fig. 3. The 3D model assembly was imported to ADAMS for the kinematic analysis. The constraints and kinematic pairs were set as well as the motion and driving force were also applied to the model before the computational simulations. Fig. 4 shows the kinematics model of the crankshaft assembly in the reciprocating compressor.

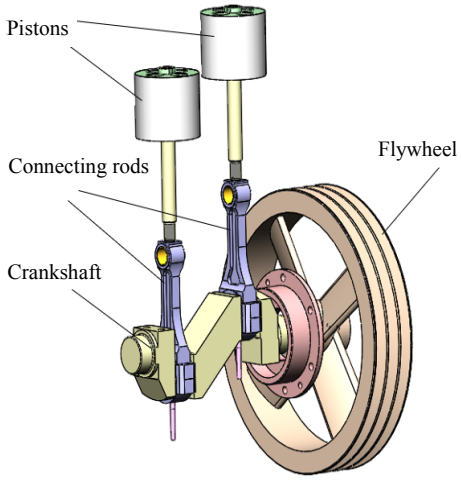

Fig. 3. 3D model of the crank-rod mechanism

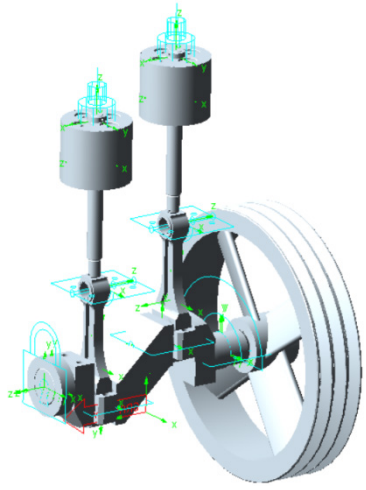

Fig. 4. Crank-rod mechanism in ADAMS

As multibody simulation software, ADAMS, can be easily integrated with the common CAD and Finite Element Analysis programs for improved results and vi-

sualization. The piston displacements plot is illustrated in Fig. 5; the moment when Piston-1 starts to move downwards from the maximum upper position manifests the start of the suction process. At the same time, Piston-2 starts moving upward from the minimum lower position, depicting the start of the exhaust process. The plot (Fig. 5) indicates the overall process during the suction and exhaust strokes of the two pistons. In this study, a two-cylinder in-line reciprocating compressor is considered; therefore, blue and red curves in Fig. 5 represent each piston's displacement time variations in one working cycle. It can be observed that two-piston displacement curves are symmetric with respect to the time axis demonstrating the alternating movement of the pistons.

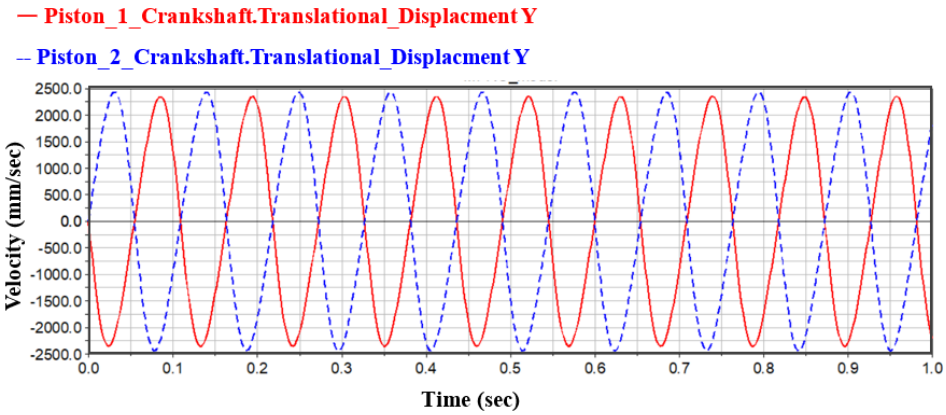

Fig. 5. Displacement-time curve of the pistons

Angular velocity and acceleration time variations for one complete working cycle of Piston-1 are illustrated in Fig. 6. The piston velocity increases from the lower dead center marking the beginning of the exhaust process (red color curve

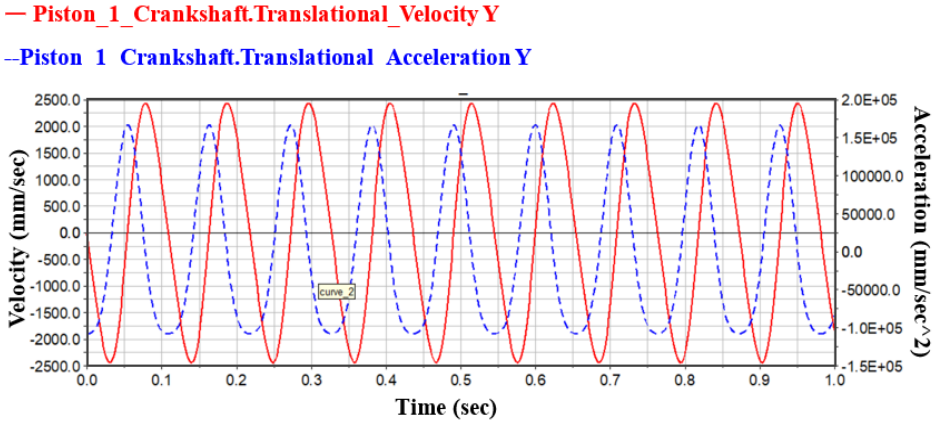

Fig. 6. Pistons velocity-time curve

in Fig. 6). It is to be noted that the negative sign in the velocity axis is only for the direction while the magnitude of the velocity increases. The acceleration produced due to this change in velocity will be neutralized (equal to zero) when the gas force from the cylinder becomes equal to the piston force at some point in the exhaust process (blue color curve in Fig. 6). There will be a continuous deceleration of the piston till it reaches the top dead center at the end of the exhaust process, i.e., at the point when the acceleration reaches zero. A similar mechanism can be justified for the Piston-2.

4. Structural analysis

4.1. Grid generation

The finite element crankshaft model was developed in ANSYS. Due to the complicated configuration structure of the crankshaft and the complexity in meshing and calculations, the oil-hole and minor fillets, which do not affect the analysis results, were omitted from the crankshaft model. The hexahedral mesh elements were used for the load and boundary application regions such as main and rod journals; hexahedral meshing is more suitable for the accuracy of the analysis where loads are applied. Tetrahedral meshing was adopted for the remaining regions including crank web parts, due to its simplicity and adoptive quality to complex geometries. The overall mesh consists of 77658 elements and 125731 nodes; the mesh scheme of the crankshaft is illustrated in Fig. 7.

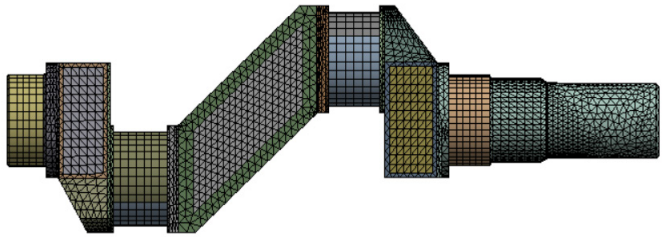

Fig. 7. Grid scheme for the crankshaft model

4.2. Static structural analysis

Static structural analysis is frequently carried out for steady loads, stress analysis, deformation, and strain on the structures or components. It is beneficial for the gradual and slow-acting structural loads irrelevant to a time dependency. For the static analysis of the original crankshaft considered in this study, the two main journals are fixed as per the real operating conditions (Fig. 2). The piston applies force on the two-rod journals through the connecting rod; this force is then used for the calculation of the load distribution by using the equivalent calculation

method. Steady-state static analysis was performed in ANSYS, where the loading was applied in terms of inertial forces, which were calculated from the gravity and rotational velocity. The load is applied to the crankshaft journal while the driving moment was applied through the flywheel at the right side of the crankshaft. Along the axis, the surface loading is assumed to be distributed parabolically, while along the circumferential direction the surface loading varies as a cosine function which is expressed in Eq. (1) [25].

$$q_{x,\theta} = \frac{9Q_c}{16LR}\left(1 - \frac{x^2}{L^2}\right)\cos\left(\frac{3\theta}{2}\right). \tag{1}$$

Equation (1) is symmetric with variables x and θ. For the application of the distributed surface load, ANSYS Parametric Design Language (APDL) module was utilized. The application of the distributed load on the crankshaft journal is demonstrated in Fig. 8, where the maximum load value is located at the mid-point of the journal surface. Additionally, loads are symmetric along the radial and axial directions on the journal surface and decrease with the distance increasing from the mid-point, hence confirming the fact expressed in Eq. (1).

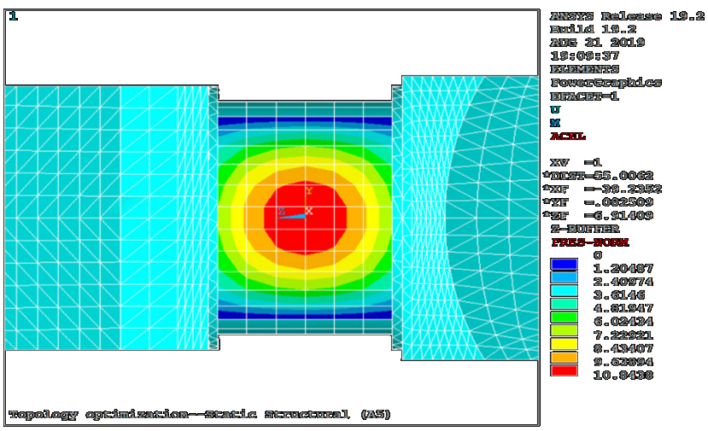

Fig. 8. Load distribution application on journal surface

The results of the deformation and stress distribution of the crankshaft are illustrated in Fig. 9 and Fig. 10. Results are obtained for the two working conditions; the first working condition refers to the highest position attained by the left rod journal when it experiences the maximum load from the piston, whereas the second working position is the highest attained position of the right rod journal when it encounters the maximum load from the piston. In the first working condition, the maximum stress (51.9 MPa) is located on the fillet between the left main journal and the crank web part, as observed in Fig. 9a. The maximum deformation (0.0086 mm) appears on the left rod journal, as illustrated in Fig. 9b. Similarly, in the second work condition, when the load is maximum on the right rod journal, the maximum

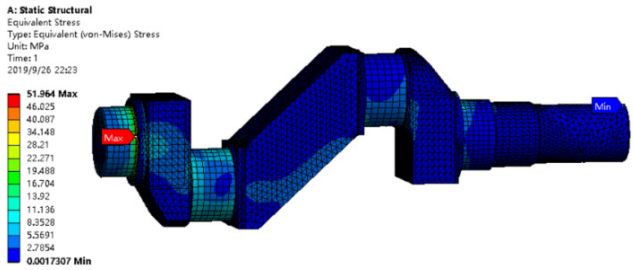

(a) Stress distribution

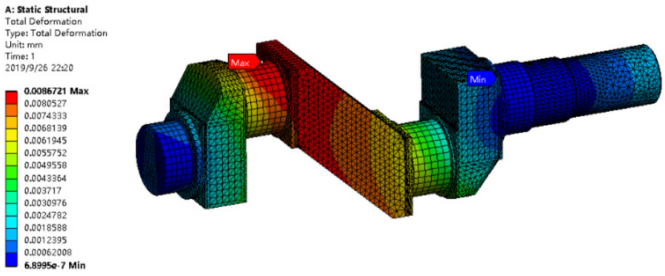

(b) Deformation distribution

Fig. 9. First working condition on the original crankshaft model

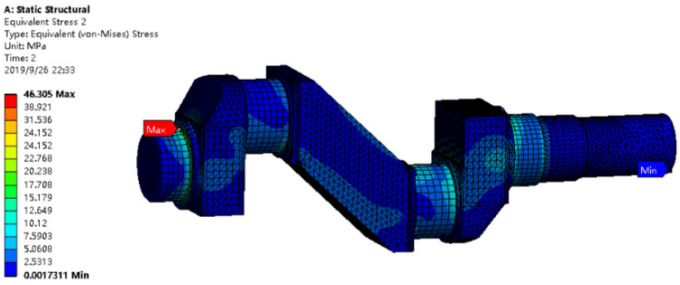

(a) Stress distribution

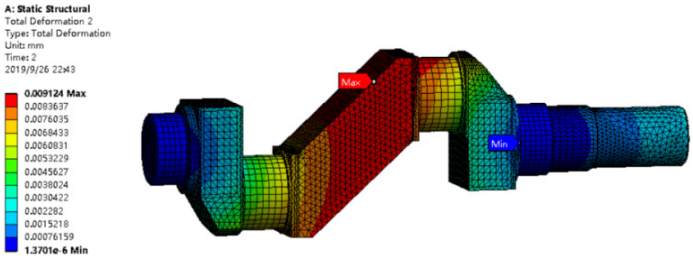

(b) Deformation distribution

Fig. 10. Second working condition on the original crankshaft model

stress (46.3 MPa) is still observed at the fillet between the left main journal and the crank web. However, the deformation location had been moved slightly towards the middle crank web part (approximately 0.009 mm), which can be ignored. The results of the static structural analysis of the crankshaft manifest that the maximum stress values are much lower than the material yield strength of the crankshaft, which implies the presence of enormous improvement potential for the original crankshaft model.

4.3. Fatigue analysis

The crankshaft experiences long-term cyclic loading during the working process, and due to the bending and torsional loads, significant stress effects can be induced in the system. In addition, dynamic load in a rotational system because of the torsional effects also exerts bending and shear stresses, which are most frequently experienced by the crankshaft and are commonly responsible for crankshaft fatigue failure. Therefore, fatigue failure is one of the core concerns in the crankshaft design and optimization. Many researchers, including Ref. [26], observed that the crankshaft fracture was mainly located at the transition area of the main shaft and crankpin.

In this section, fatigue analysis of the original crankshaft model is presented; Finite Element Method (FEM) was utilized to predict and estimate the crankshaft fatigue life by using the fatigue analysis module Ncode Design Life in ANSYS. The fatigue analysis consists of three primary input parameters, i.e., Finite Element (FE) results, Material Mapping, and Load Mapping. Fig. 11 illustrates the layout of the fatigue analysis methodology adopted for this study.

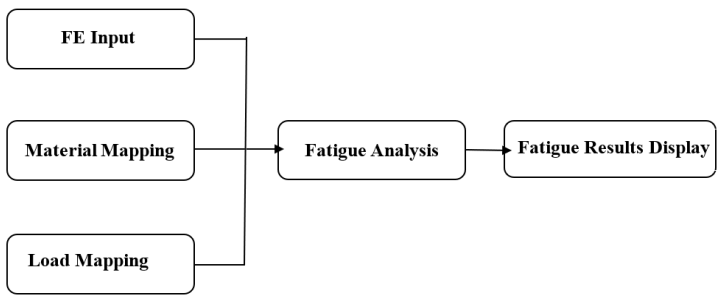

Fig. 11. Layout of the fatigue analysis methodology

The fatigue analysis is performed after the static analysis; therefore, the static analysis results are considered as the input parameters for the fatigue analysis. In the static analysis, two working conditions were analyzed; because of this reason, the time-step method was utilized as the load mapping input parameter for the fatigue analysis. Material parameters of SAE 1045 steel were used as the input in the material editor Ncode. Fig. 12 illustrates the flow chart of the fatigue analysis.

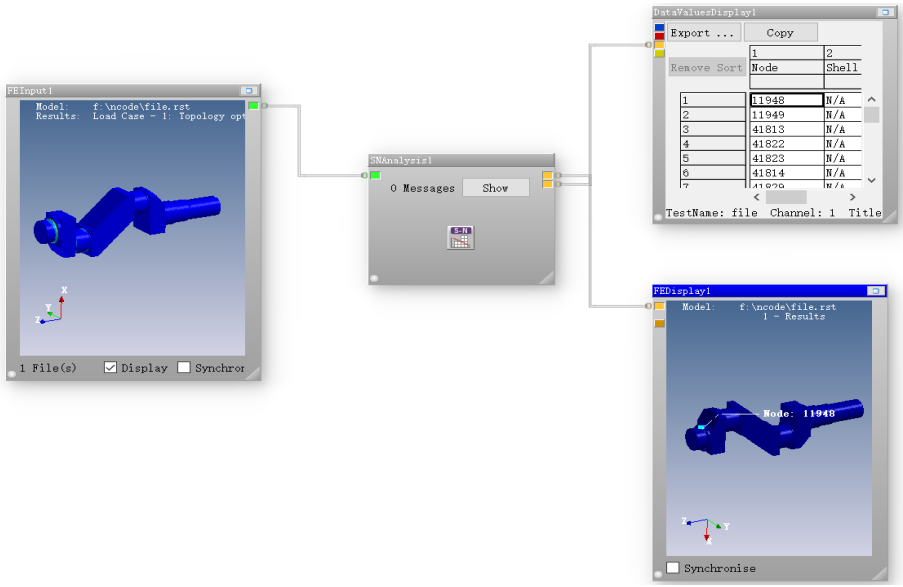

Fig. 12. Flow chart of the fatigue analysis method in Ncode

The fatigue analysis results in terms of the total life contour of the crankshaft are demonstrated in Fig. 13. The red color in the contour plot indicates critical regions in the crankshaft, whereas the blue color indicates the values below the endurance limit. Ref. [27] suggested that fatigue failure could be ignored after

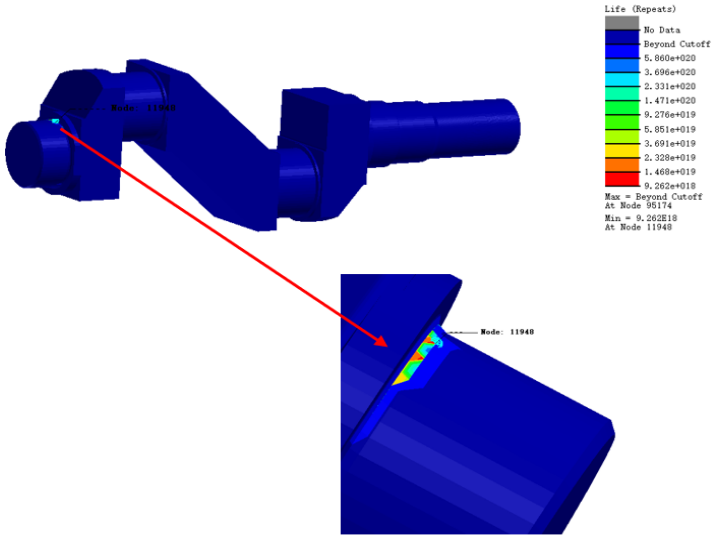

Fig. 13. Fatigue life of the original crankshaft model

8.0e+6 cycles. In this study, the minimum value observed for the crankshaft fatigue life is 9.26e+018 which is much higher than the reference value (8.0e+6) indicated in [27]; therefore, the crankshaft can be regarded as infinite fatigue strength. The minimum cycle value is observed at the fillet between the left main journal and crank web (Fig. 13), which is due to the maximum stresses acting at the fillet, also observed in the static analysis. From the fatigue results, it can be concluded that the fillet between the left main journal and crank web is the weakest location on the crankshaft; however, the value of fatigue obtained from the analysis is far more secure than the default value, and the crankshaft can operate without any alarming condition.

5. Topology optimization

In recent years, topology optimization has gained significant importance among researchers and engineers for the optimal layout of the structures in the design regions. Cost-effectiveness, ease of implementation, and efficiency in the analysis of structures and mechanisms are the main benefits of topology optimization. In this study, topology optimization is used to achieve the crankshaft weight reduction goal while keeping the strength under acceptable and safe limits. Topology optimization is a well-established mathematical method; the general optimization expression is provided in [28] and represented here in terms of Eq. (2).

$$\begin{aligned} &\text{Min}\,(f(x)) \\ &\text{Subjected to:} \quad g_j(x) \leqslant 0 \qquad\qquad j = 1,\ldots,m_g \\ &\qquad\qquad\quad h_k(x) = 0 \qquad\qquad k = 1,\ldots,m_k \\ &\qquad\qquad\quad x_{i,\min} \leqslant m_g \leqslant x_{i,\max} \quad i = 1,\ldots,n \end{aligned} \tag{2}$$

where, x is the vector of design variables within the predefined permissible range, $f(x)$ is the objective function, $g_j(x)$ and $h_k(x)$ are the inequality and equality constraints, respectively.

Since the interchangeability precondition of the crankshaft is one of the main objectives of the optimization, the three crank web parts were chosen as the design regions for topology optimization. Crank webs are the ultimate choice for the topology optimization as the hollow design should be implemented to crank webs only; hence, by doing so, the overall weight reduction can be achieved. On the other hand, hollow design for the other parts such as main or rod journals is not suitable as the main stresses are applied on these parts and in the case of hollow design the strength will be compromised, which is not an option for the crankshaft smooth performance.

Fig. 14 illustrates the topology optimization results obtained after the analysis of three crank webs. Considering the retention ratio and the symmetric constraints, the optimization process was analyzed in ANSYS. The final material retention-ratio

range of the design region was kept from 0.6 to 1 because only within this range the crank webs material was flexible in terms of strength and smooth operation of the crankshaft. From the analysis, it was observed that a range lower than 0.6 would cause an overall low crankshaft thickness and strength, which would critically affect the crankshaft performance. Topology optimization possesses a unique advantage of the highest possibility of continuous improvement in design; for instance, the retention ratio and the symmetric constraints are flexible and can be altered depending upon the type and design of the crankshaft. Additionally, due to the topology optimization, improved results in terms of mechanical properties can be obtained; material removal ensures not only the weight reduction but also the manufacturing cost.

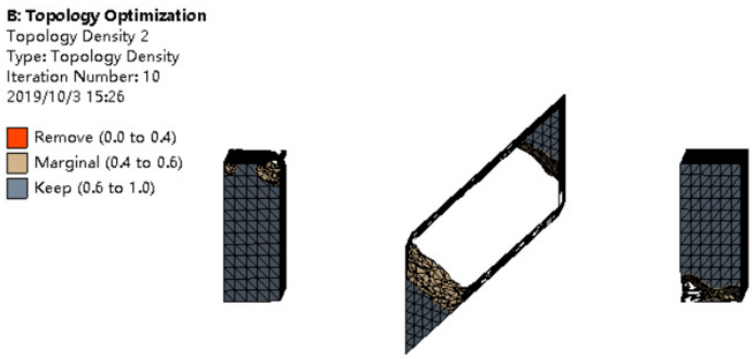

Fig. 14. Topology optimization of three crankshaft crank webs

Topology optimization in this study manifests an impressive weight reduction ranging from 14738 to 12839 grams, which is equal to approximately 13% material removal from the original crankshaft. Fig. 15 demonstrates the crankshaft model after the topology optimization; it can be observed that a considerable amount of material has been removed from the crankshaft; hence, the core aim of lightweight crankshaft design is achieved. The mechanical properties of the optimized crankshaft after the material retention must be re-observed and compare with the original crankshaft models. This comparison is presented in the next section.

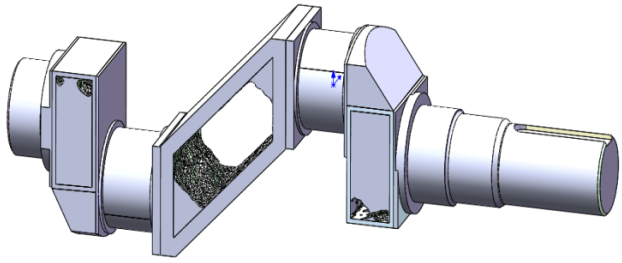

Fig. 15. Optimized crankshaft model

6. Results comparison

For better understanding of the results and optimization analysis so far, Static Analysis and Topology Analysis are briefly compared here:

6.1. Mass reduction

Fig. 16 shows the comparison of the original crankshaft model and the optimized model. As mentioned earlier, there is a total mass reduction of approximately 13% after the optimization.

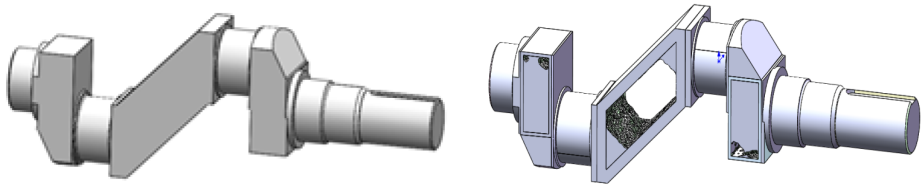

(a) Original model (b) Optimized model

Fig. 16. Optimized crankshaft model

6.2. General stress and deformation distribution

After the topology optimization, a static analysis was performed on the optimized crankshaft model with the same loads and boundary conditions as those of the original model. Figs. 17, 18 compare the stress and deformation distribution of the optimized model with the original model. In the first working condition (left rod journal with maximum load), both original and optimized models experience the maximum stress at the junction between the left main journal and crank web, as shown in Fig. 17. In order to relieve the stress concentration effect on the fillet, Ref. [29] suggested to increase the fillet radius. This technique was adopted for the optimized crankshaft, and the fillet radius was enlarged from 5 mm to 9 mm. As a result, the optimized crankshaft stress concentration was relieved in the first as well as in the second working condition. For the first work cycle, the maximum stress value had been dropped from 51.364 MPa to 49.603 MPa (Fig. 17b). Fig. 18 illustrates the comparison of the deformation distribution on the crankshaft for the first working condition. There is a slight increase in the maximum value of the deformation distribution (0.0086 mm to 0.0106 mm); such a minor deformation does not affect the crankshaft operation and can be ignored.

Figs. 19, 20 present the stress and deformation distribution for the second working condition (right rod journal with maximum load). The maximum stress is on the fillet between the left main journal and the crank web, which has been reduced from 46.305 MPa to 45.182 MPa in the optimized model as compared to

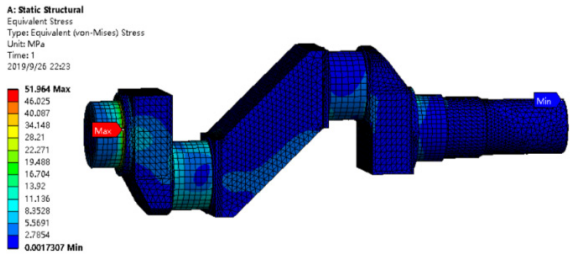

(a) Original model

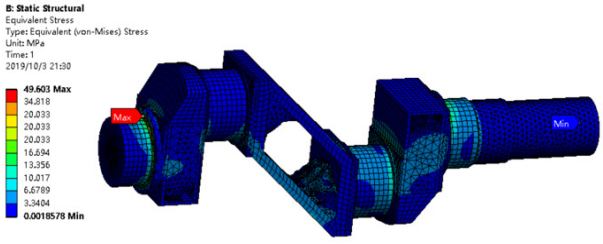

(b) Optimized model

Fig. 17. Stress distribution of first working condition

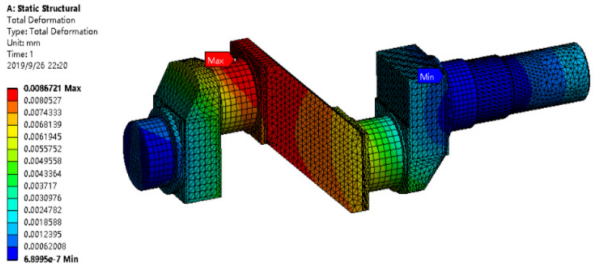

(a) Original model

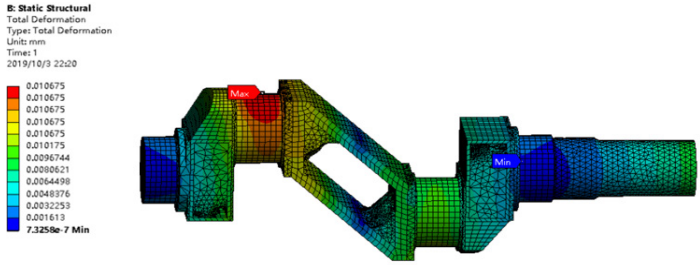

(b) Optimized model

Fig. 18. Deformation distribution of first working condition

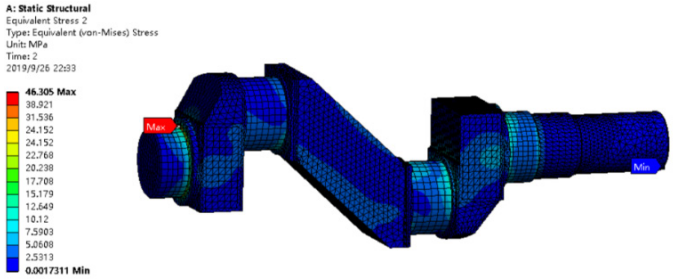

(a) Original model

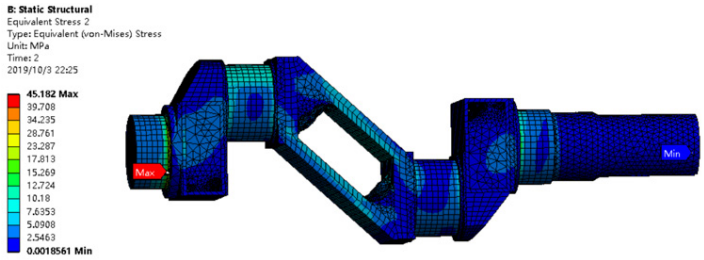

(b) Optimized model

Fig. 19. Stress distribution of second working condition

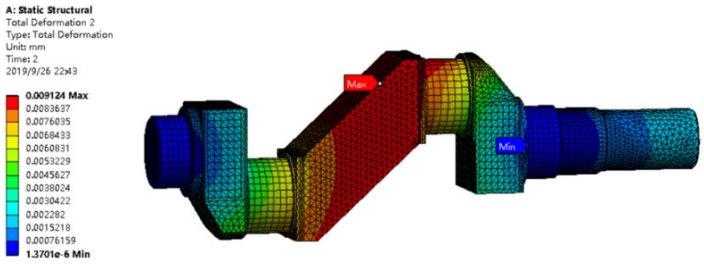

(a) Original model

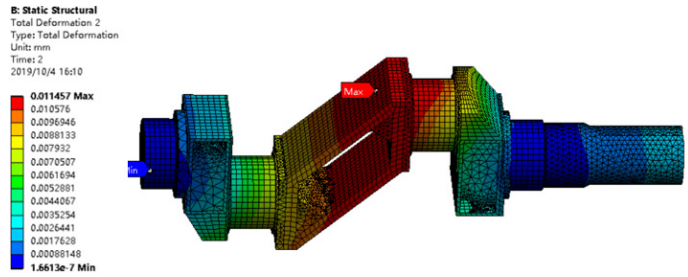

(b) Optimized model

Fig. 20. Deformation distribution of second working condition

the original model respectively (Fig. 19). Similar to the first working condition, there was a minor increase in the deformation distribution (0.002 mm) in the optimized design, which is negligible and can be ignored.

Crankshaft optimization in terms of weight reduction and mechanical properties is the main aim of this study. From the results obtained so far, comparison based on the static and topology optimization, the goal of the study has been achieved as a significant amount of weight was reduced. In addition, the crankshaft stress concentration also improved while the deformation distribution remained nearly unchanged. Although the optimization results are satisfactory, it would be better not solely rely on the static optimization results. Therefore, for further comparison/verification of the static analysis and improved results, dynamic modal analysis (for the dynamic characteristics) was performed and presented in the following section.

7. Dynamic modal analysis

Modal analysis can provide the basic dynamic characteristics of the structure. For the design optimization, the modal analysis is frequently utilized to observe the natural frequency of the model and avoid the coincidence with the frequency of the excitation forces, i.e., to avoid the resonance effects as much as possible. To examine the optimized crankshaft time-dependent dynamic characteristics, modal analysis is additionally performed in this study. Dynamic modal analysis was carried out in ANSYS, and the natural frequency of the free modes of the optimized crankshaft was calculated. Table 3 presents the 6-order natural frequency of the crankshaft.

Table 3.

Crankshaft modal frequency

Mode	Frequencies FEA (Hz)
1	24.21
2	1250.70
3	2426.70
4	2460.41
5	2469.86
6	3714.10

The 6-order free modes of the crankshaft are illustrated in Figs. 21–26. Fig. 21 and Fig. 22 are the 1st and the 2nd order twisting modes along z-axis, respectively; the maximum displacements are on the middle crank web. In Figs. 23– 24, the 3rd and the 4th vibration mode results are similar where the maximum displacements are located on the right end of the crankshaft; however, the bending is along the x-axis. 5th natural frequency mode oscillations are along the z-axis, and the maximum displacement is located on the right end of the crankshaft at the main journal, as indicated in Fig. 25. Fig. 26 shows the 6th order natural frequency mode, which

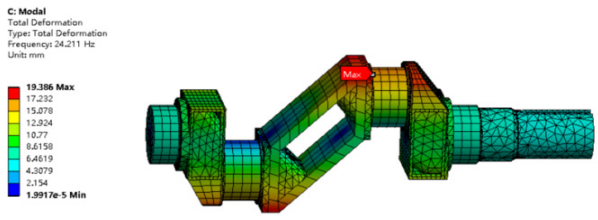

Fig. 21. First order natural frequency of the optimized crankshaft

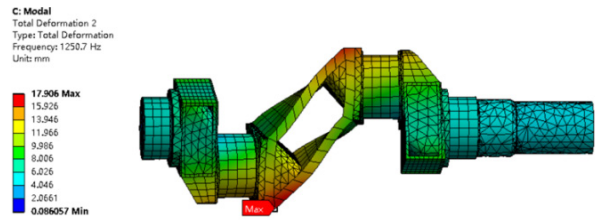

Fig. 22. Second order natural frequency of the optimized crankshaft

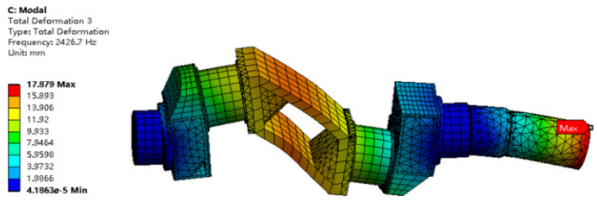

Fig. 23. Third order natural frequency of the optimized crankshaft

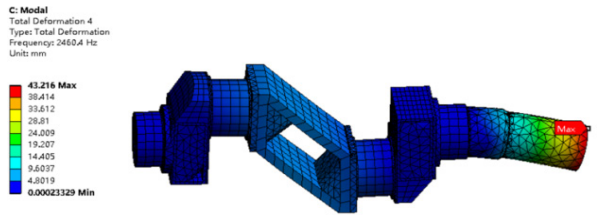

Fig. 24. Forth order natural frequency of the optimized crankshaft

is the combination vibration mode, i.e., twist along the x-axis and swings at both ends of the crankshaft. The maximum displacement is observed at the left crank web.

From the modal analysis results, information about the vibration type and frequency of the modes can be obtained. These results are useful for the optimization period to avoid matching with the excitation forces, i.e., resonance.

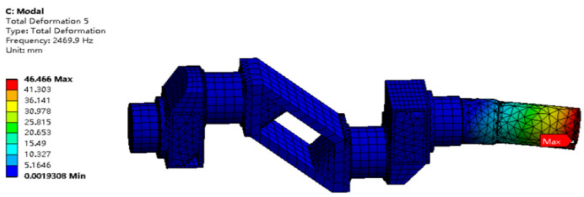

Fig. 25. Fifth order natural frequency of the optimized crankshaft

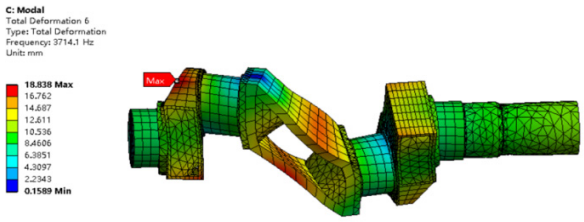

Fig. 26. Sixth order natural frequency of the optimized crankshaft

8. Discussion

This study was aimed at optimizing the two-cylinder in-line reciprocating compressor crankshaft. Weight reduction with improved mechanical properties was set as the core objective of the crankshaft design optimization process, which was achieved by carrying out kinematic, static, fatigue, topology, and dynamic modal analysis. The results of the design optimization process demonstrate a prominent amount of crankshaft weight reduction. The optimized crankshaft is approximately 13% lighter as compared to the original crankshaft model. Crankshaft optimization is frequently considered a complex process where weight loss in some cases is achieved at the cost of mechanical properties; however, in this study, the weight reduction is attained along with the improved mechanical properties. As a result, stress concentration was improved at the critical vicinity of the junction between the left main journal and crank web; additionally, the overall stress distribution on the crankshaft was also improved. Cost reduction is another beneficial aspect of the optimization analysis, and the material retention achieved during the topology optimization can imply a significant future manufacturing cost reduction of the crankshaft.

The ZW series of reciprocating compressors is one of the most operational series in the industry and will remain in use in the future as well; therefore, the optimization of this compressor crankshaft can be wildly applied to reduce manufacturing cost on a large scale. Furthermore, this optimization study is not limited to this compressor type but is also applicable to heavy-duty reciprocating compressors and engines with multi-cylinder design, as well as for the stress analysis of non-rotating and rotating machine parts such as rollers and bearings. The implication of this study is not limited to the industry, but it also can contribute

to the research fields. The stress analysis methodology developed for this study will be further utilized for the design of wind tunnel structural elements, wings of test aircraft, and nozzle structures for aerospace applications, etc., under the ERDF (European Regional Development Fund) project of which this study is a part. Besides wing tunnel applications, the authors are planning to use the findings of this study for the topology optimization of the aircraft wings.

The following aspects of the current study will be explored further in the coming future:

1. Transient analysis of the optimized crankshaft model for further investigation of the dynamic characteristics.
2. The analysis of vibration, noise, and imbalance effects.
3. As a final step, testing the final optimized crankshaft model in the actual machine for the result verification.

9. Conclusion

The following conclusions can be drawn from the study:

- Approximately 13% of weight reduction was achieved after the optimization.
- The overall stress concentration was relieved, and the crankshaft working performance improved due to the stress distributions on the crankshaft.
- The design optimization in this study fulfills the interchangeability condition, i.e., the optimized crankshaft can be replaced with the original crankshaft without any additional component requirement in the system.
- This study provides an exact 3D optimized model with complete design features, which can add convenience in manufacturing the crankshaft, unlike other optimization studies, where only a few geometric parameters are provided, which often lead to manufacturing constraints and difficulties.
- The optimized crankshaft model can be a potential candidate for the two-cylinder inline ZW series mechanical design and performance modifications. Furthermore, the methodology used in this study for design optimization can further be utilized to resolve structural and design issues of several fields, including reciprocating compressors/engines, mechanical/structural equipment, piping, and aerospace industry.

Acknowledgements

This work has been supported by the European Regional Development Fund within the Activity 1.1.1.2 “Post-doctoral Research Aid” of the Specific Aid Objective 1.1.1 “To increase the research and innovative capacity of scientific institutions of Latvia and the ability to attract external financing, investing in human resources and infrastructure” of the Operational Program “Growth and Employment” (No. 1.1.1.2/VIAA/2/18/321).

Manuscript received by Editorial Board, May 28, 2021;
final version, September 16, 2021.

References

[1] Z.P. Mourelatos. A crankshaft system model for structural dynamic analysis of internal combustion engines. *Computers & Structures*, 79(20-21):2009–2027, 2001. doi: 10.1016/S0045-7949(01)00119-5.

[2] A.P. Druschitz, D.C. Fitzgerald, and I. Hoegfeldt. Lightweight crankshafts. SAE Technical Paper 2006-01-0016, 2006. doi: 10.4271/2006-01-0016.

[3] K. Mizoue, Y. Kawahito, and K. Mizogawa. Development of hollow crankshaft. *Honda R&D Technical Review 2009*, pages 243–245, 2009.

[4] I. Papadimitriou and K. Track. Lightweight potential of crankshafts with hollow design. *MTZ Worldwide*, 79:42–45, 2018. doi: 10.1007/s38313-017-0140-8.

[5] M. Roeper and S. Reinsch. Hydroforging: a new manufacturing technology for forged lightweight products of aluminum. *Proceedings of the ASME 2005 International Mechanical Engineering Congress and Exposition. Manufacturing Engineering and Materials Handling, Parts A and B*, pages 297-304. Orlando, Florida, USA, November 5–11, 2005. doi: 10.1115/IMECE2005-80424.

[6] J. Lampinen. Cam shape optimization by genetic algorithm. *Computer-Aided Design*, 35(8):727–737. doi: 10.1016/S0010-4485(03)00004-6.

[7] A. Albers, N. Leon, H. Aguayo, and T. Maier. Multi-objective system optimization of engine crankshafts using an integration approach. *Proceedings of the ASME 2008 International Mechanical Engineering Congress and Exposition. Volume 14: New Developments in Simulation Methods and Software for Engineering Applications*, pages 101–109. Boston, Massachusetts, USA. October 31–November 6, 2008. doi: 10.1115/IMECE2008-67447.

[8] J.P. Henry, J. Topolsky, and M. Abramczuk. Crankshaft durability prediction – a new 3-D approach. SAE Technical Paper 920087, 1992. doi: 10.4271/920087.

[9] M. Guagliano, A. Terranova, and L. Vergani. Theoretical and experimental study of the stress concentration factor in diesel engine crankshafts. *Journal of Mechanical Design*, 115(1):47–52, 1993. doi: 10.1115/1.2919323.

[10] A.C.C. Borges, L.C. Oliveira, and P.S. Neto. Stress distribution in a crankshaft crank using a geometrically restricted finite element model. SAE Technical Paper 2002-01-2183, 2002. doi: 10.4271/2002-01-2183.

[11] D. Taylor, W. Zhou, A.J. Ciepalowicz, and J. Devlukia. Mixed-mode fatigue from stress concentrations: an approach based on equivalent stress intensity. *International Journal of Fatigue*, 21(2):173–178, 1999. doi: 10.1016/S0142-1123(98)00066-8.

[12] W. Li, Q. Yan, and J. Xue. Analysis of a crankshaft fatigue failure. *Engineering Failure Analysis*, 55:13-9-147, 2015. doi: 10.1016/j.engfailanal.2015.05.013.

[13] R.M. Metkar, V.K. Sunnapwar, and S.D. Hiwase. Comparative evaluation of fatigue assessment techniques on a forged steel crankshaft of a single cylinder diesel engine. *Proceedings of the ASME 2012 International Mechanical Engineering Congress and Exposition. Volume 3: Design, Materials and Manufacturing, Parts A, B, and C*, pages 601–609. Houston, Texas, USA, November 9–15, 2012. doi: 10.1115/IMECE2012-85493.

[14] Y. Shi, L. Dong, H. Wang, G. Li, and S. Liu. Fatigue features study on the crankshaft material of 42CrMo steel using acoustic emission. *Frontiers of Mechanical Engineering*, 11(3):233–241, 2016. doi: 10.1007/s11465-016-0400-3.

[15] J. Yao and J. Zhang. A modal analysis for vehicle's crankshaft. *2017 IEEE 3rd Information Technology and Mechatronics Engineering Conference*, pages 300–303, 2017. doi: 10.1109/ITOEC.2017.8122303.

[16] A.S. Mendes, E. Kanpolat, and R. Rauschen. Crankcase and crankshaft coupled structural analysis based on hybrid dynamic simulation. *SAE International Journal of Engines*, 6(4):2044–2053, 2013. doi: 10.4271/2013-01-9047.

[17] B. Yu, Q. Feng, and X. Yu. Dynamic simulation and stress analysis for reciprocating compressor crankshaft. *Proceedings of the Institution of Mechanical Engineers, Part C: Journal of Mechanical Engineering Science*, 227(4):845–851, 2013. doi: 10.1177/0954406212453523.

[18] A. Arshad, S. Samarasinghe, M.A.F. Ameer, and A. Urbahs. A simplified design approach for high-speed wind tunnels. Part I: Table of inclination. *Journal of Mechanical Science and Technology*, 34(6):2455–2468, 2020. doi: 10.1007/s12206-020-0521-9.

[19] A. Arshad, S. Samarasinghe, and V. Kovalcuks. A simplified design approach for high-speed wind tunnels. Part-I.I: Optimized design of settling chamber and inlet nozzle. *2020 11th International Conference on Mechanical and Aerospace Engineering (ICMAE)*, pages 150–154, 2020. doi: 10.1109/ICMAE50897.2020.9178865.

[20] A. Arshad, M.A.F. Ameer, and O. Kovzels. A simplified design approach for high-speed wind tunnels. Part II: Diffuser optimization and complete duct design. *Journal of Mechanical Science and Technology*, 35(7):2949–2960, 2021. doi: 10.1007/s12206-021-0618-9.

[21] A. Arshad, N. Andrew, and I. Blumbergs. Computational study of noise reduction in CFM56-5B using core nozzle chevrons. *2020 11th International Conference on Mechanical and Aerospace Engineering (ICMAE)*, pages 162-167, 2020. doi: 10.1109/ICMAE50897.2020.9178891.

[22] A. Arshad, L.B. Rodrigues, and I.M. López. Design optimization and investigation of aerodynamic characteristics of low Reynolds number airfoils. *International Journal of Aeronautical and Space Sciences*, 22:751–764, 2021. doi: 10.1007/s42405-021-00362-2.

[23] A. Arshad, A.J. Kallungal and A.E.E.E. Elmenshawy. Stability analysis for a concept design of Vertical Take-Off and Landing (VTOL) Unmanned Aerial Vehicle (UAV). *2021 International Conference on Military Technologies (ICMT)*, pages 1–6, 2021. doi: 10.1109/ICMT52455.2021.9502764.

[24] RanTong official database for the ZW-0.8/10-16 reciprocating compressor specifications, online resources.

[25] F. Rodriges Minucci, A.A. dos Santos, and R.A. Lime e Silva. Comparison of multiaxial fatigue criteria to evaluate the life of crankshafts. *Proceedings of the ASME 2010 International Mechanical Engineering Congress and Exposition. Volume 11: New Developments in Simulation Methods and Software for Engineering Applications; Safety Engineering, Risk Analysis and Reliability Methods; Transportation Systems*, pages 775–784. Vancouver, British Columbia, Canada. November 12–18, 2010. doi: 10.1115/IMECE2010-39018.

[26] Y.F. Sun, H.B. Qiu, L. Gao, K. Lin, and X.Z. Chu. Stochastic response surface method based on weighted regression and its application to fatigue reliability analysis of crankshaft. *Proceedings of the ASME 2009 International Mechanical Engineering Congress and Exposition. Volume 13: New Developments in Simulation Methods and Software for Engineering Applications; Safety Engineering, Risk Analysis and Reliability Methods; Transportation Systems*, pages 263-268. Lake Buena Vista, Florida, USA. November 13–19, 2009. doi: 10.1115/IMECE2009-11095.

[27] Y. Gorash, T. Comlekci, and D. MacKenzie. Comparative study of FE-models and material data for fatigue life assessments of welded thin-walled cross-beam connections. *Procedia Engineering*, 133:420–432, 2015. doi: 10.1016/j.proeng.2015.12.612.

[28] C. Cevik and E. Kanpolat. Achieving optimum crankshaft design – I. SAE Technical Paper 2014-01-0930, 2014. doi: 10.4271/2014-01-0930.

[29] G. Mu, F. Wang, and X. Mi. Optimum design on structural parameters of reciprocating refrigeration compressor crankshaft. *Proceedings of the 2016 International Congress on Computation Algorithms in Engineering*, pages 281–286, 2016. doi: 10.12783/dtcse/iccae2016/7204.